Redox Potential Difference between *Desulfovibrio vulgaris* and *Clostridium beijerinckii* Flavodoxins[†]

Hiroshi Ishikita*

417 SGM Building, Department of Chemistry, University of Southern California, Los Angeles, California 90089

Received October 26, 2007; Revised Manuscript Received January 30, 2008

ABSTRACT: The redox potential of the flavin mononucleotide (FMN) hydroquinones for one-electron reduction in the *Desulfovibrio vulgaris* (*D. vulgaris*) flavodoxin ($E_{sq/hq}$ for $FMNH^{\bullet}/FMNH^{-}$) was calculated using the crystal structure of the relevant hydroquinone form and compared to the results of the *Clostridium beijerinckii* (*C. beijerinckii*) flavodoxin. In *D. vulgaris* and *C. beijerinckii* flavodoxins, the protein side chain causes significant downshifts of 170 and 240 mV in $E_{sq/hq}$, respectively. In the *C. beijerinckii* flavodoxin, the $E_{sq/hq}$ downshift because of the protein side chain is essentially compensated by the counter influence of the protein backbone ($E_{sq/hq}$ upshift of 260 mV). However, in the *D. vulgaris* flavodoxin, the corresponding protein backbone influence on $E_{sq/hq}$ is significantly small, i.e., less than half of that in the *C. beijerinckii* flavodoxin. In particular, there is a significant difference in the influence of the protein backbone of the so-called 60s loop region between the two flavodoxins. The $E_{sq/hq}$ difference can be best explained by the lower compensation of the side chain influence by the backbone influence in the *D. vulgaris* flavodoxin than in the *C. beijerinckii* flavodoxin.

The redox-active protein flavodoxin has a quinone molecule flavin mononucleotide (FMN),[1] which functions as a redox-active group. The oxidized (OX) quinone (FMN) can be reduced to the hydroquinone (HQ) anion ($FMNH^{-}$), while reduction of the HQ occurs via semiquinone (SQ) anion ($FMN^{\bullet -}$) or semiquinone neutral ($FMNH^{\bullet}$) (*1, 2*). Thus, they show two characteristic redox potentials (E_m),[2] namely, $E_{sq/hq}$ and $E_{ox/sq}$ (*3*). $E_{sq/hq}$ represents the E_m for one-electron reduction from $FMNH^{\bullet}$ to $FMNH^{-}$ [i.e., $E_m(FMNH^{\bullet}/FMNH^{-})$]. On the other hand, $E_{ox/sq}$ represents the E_m for proton-coupled one-electron reduction from FMN to $FMNH^{\bullet}$ [i.e., E_m(FMN/$FMNH^{\bullet}$)]. It has been widely observed that, in contrast to the $E_{sq/hq}$ values, mutations of charged to uncharged residues in flavodoxins do not clearly correlate with the $E_{ox/sq}$ values (*4, 5*). Redox reactions of flavins in protein environments have also been studied with computational methods (e.g., see refs *2, 6, and 7*). In the previous computational study on redox potentials of the *Clostridium beijerinckii*flavodoxin (*7*), we successfully reproduced the experimentally measured values using the atomic coordinates of the crystal structures in their relevant forms [i.e., the hydroquinone form for $E_{sq/hq}$ and the HQ and oxidized (OX) forms for $E_{ox/sq}$ (*8*)]. It demonstrated that the redox potential and pK_a values of groups embedded in the protein can be accurately predicted from the protein structure data (i.e., atomic coordinates) alone (*7*).

In the present study, using crystal structures and considering the protonation states of all titratable sites (including the FMN 5′-phosphate group) in the protein, the calculated $E_{sq/hq}$ values of flavodoxins from *Desulfovibrio vulgaris* are presented. We focus on only $E_{sq/hq}$ because it is more straightforward to analyze the influence of the protein environment on $E_{sq/hq}$ than on $E_{ox/sq}$ (see refs *4, 5, and 7*). Here, we pay particular attention to the so-called 60s loop region that lies in the proximity of FMN and whose importance in tuning the redox potential has been reported (*5, 8, 9*). In addition, we investigate the role of the FMN 5′-phosphate group in $E_{sq/hq}$, which has been a matter of debate (*7, 10–14*). The computational conditions and procedures used in studies on the *C. beijerinckii* flavodoxin (*7*) were consistently used in the present study; this can facilitate the direct analysis and comparison of the influences of protein environments on $E_{sq/hq}$ in both the *D. vulgaris* and *C. beijerinckii* flavodoxins.

COMPUTATIONAL PROCEDURES

Atomic Coordinates and Charges. To perform computations of native flavodoxin, a crystal structure of the native *D. vulgaris* flavodoxin was used [Protein Data Bank (PDB) 5FX2 for the HQ form, 3FX2 for the OX form (*15*), and 1BU5 for the apoflavodoxin−riboflavin complex form (*12*)]. Calculations for obtaining $E_m(FMNH^{\bullet}/FMNH^{-})$ were performed using the HQ structures, unless otherwise specified.

The atomic coordinates were obtained using the same procedures used in previous studies on the *C. beijerinckii*

[†] H.I. is supported by the Japan Society for the Promotion of Science (JSPS) fellowship for research abroad.

* To whom correspondence should be addressed: 417 SGM Building, Department of Chemistry, University of Southern California, Los Angeles, CA 90089. Telephone: +1-213-740-7671. Fax: +1-213-740-2701. E-mail: hzi1@usc.edu.

[1] Abbreviations: *C. beijerinckii*, *Clostridium beijerinckii*; *D. vulgaris*, *Desulfovibrio vulgaris*; E_m, redox (midpoint) potential; $E_{sq/hq}$, $E_m(FMNH^{\bullet}/FMNH^{-})$; FMN, flavin mononucleotide; $FMN^{\bullet -}$, FMN semiquinone anion; $FMNH^{\bullet}$, FMN semiquinone neutral; $FMNH^{-}$, hydroquinone anion; HQ, FMN in the hydroquinone form; LPB, linear Poisson–Boltzmann; OX, FMN in the oxidized form; PDB, Protein Data Bank; 60s loop, loop region at the 60s residues.

[2] The difference of 1000 mV in redox potential (ΔE_m) yields an energy of 1000 meV ≈ 23.06 kcal/mol for an electron.

10.1021/bi702151k CCC: $40.75
Published on Web 03/21/2008

flavodoxin (*7*). The positions of H atoms were energetically optimized with CHARMM (*16*) using the CHARMM22 force field. While carrying out this procedure, the positions of all non-hydrogen atoms were fixed and the standard charge states of all of the titratable groups were maintained; i.e., basic and acidic groups were considered to be protonated and deprotonated, respectively. All of the other atoms whose coordinates were available in the crystal structure were not geometrically optimized.

Atomic partial charges of the amino acids were adopted from the all-atom CHARMM22 (*16*) parameter set. Atomic charges of the 5′-phosphate group of FMN quinone ($-H_3PO_3$, $-H_2PO_3^-$, and $-HPO_3^{2-}$) were adopted from those of the methylphosphate CHARMM22 parameter set (labeled using MP_0, MP_1, and MP_2, respectively). The charges of $FMNH^{\bullet}$ and $FMNH^-$ were quoted from a previous paper on the *C. beijerinckii* flavodoxin (*7*).

Protonation Pattern, Redox Potential, and pK_a. The present computation is based on the electrostatic continuum model created by solving the linear Poisson–Boltzmann (LPB) equation with the MEAD program (*17*). To facilitate a direct comparison to previous computational results, we uniformly used identical computational conditions and parameters, such as atomic partial charges and dielectric constants (e.g., refs *7 and 18–20*). To obtain absolute E_m values of the protein, we calculated the electrostatic energy difference between the two redox states in a reference model system using a known experimental E_m value. The difference in the E_m value of the protein relative to the reference system was added to the known E_m value. As a reference model system, the following values for E_m versus the normal hydrogen electrode (NHE) were used: $E_m(FMNH^{\bullet}/FMNH^-) = -172$ mV at pH 7 for one-electron reduction (-172 mV $= E_{sq/hq}$) measured by Draper and Ingraham with potentiometry (*21*). All of the other titratable sites, including the 5′-phosphate group, were fully equilibrated to the redox state of FMN during the titration. The ensemble of the protonation patterns was sampled by the Monte Carlo (MC) method with Karlsberg [Rabenstein, B. (1999) Karlsberg online manual, http://agknapp.chemie.fu-berlin.de/karlsberg/]. The dielectric constants were set to $\epsilon_p = 4$ inside the protein and $\epsilon_w = 80$ for water. All computations were performed at 300 K, pH 7.0, and an ionic strength of 100 mM. The LPB equation was solved using a three-step grid-focusing procedure at the resolutions of 2.5, 1.0, and 0.3 Å. The MC sampling yielded the probabilities [A_{ox}] and [A_{red}] of the two redox states of molecule *A*. The E_m was evaluated using the Nernst equation. A bias potential was applied to obtain an equal amount of both redox states ([A_{ox}] = [A_{red}]), thereby yielding the redox midpoint potential E_m as the resulting bias potential. For convenience, the computed E_m value was given with millivolt accuracy, without implying that the last digit was significant. In general, an E_m value of approximately 10 mV is a sufficiently reproducible range for the computational method used (e.g., refs *7 and 18–20*). The value of 6.4 (*22*) was considered as the pK_a value of the 5′-phosphate group of $-H_2PO_3^-/-HPO_3^{2-}$. Note that the 5′-phosphate group was permanently deprotonated in the $-H_3PO_3/-H_2PO_3^-$ equilibrium [pK_a = 1.4 (*22*)] in all of the crystal structures that were investigated. Thus, in the present study, the $-H_2PO_3^-/-HPO_3^{2-}$ equilibrium [pK_a = 6.4 (*22*)] was investigated, unless otherwise specified.

Reference E_m Values in the Reference Model System. In the present study, the $E_{sq/hq}$ value of -172 mV for free FMN measured by Draper and Ingraham by potentiometry (*21*) was tentatively used as in previous studies on the *C. beijerinckii* flavodoxin (*7*) [note that $E_{ox/sq} = -238$ mV (*21*), although not used in the present study]. On the other hand, the corresponding value measured by Anderson by pulse radiolysis was -124 mV (-314 mV for $E_{ox/sq}$) (*23*). More recently, by performing plot-fitting analysis of pH dependence on $E_{sq/hq}$ and $E_{ox/sq}$ obtained from earlier studies (*21, 23*), Mayhew (*24*) observed a larger deviation of the data measured by Draper and Ingraham (*21*) from those anticipated by the Michaelis equation (*25*). He concluded that the latter was more reliable. Measurements of the $E_{sq/hq}$ and $E_{ox/sq}$ values by Williamson and Edmondson (*26*) also deviate from those anticipated by the Michaelis equation. In aqueous solution, redox reactions of quinones are often coupled with protonation events, while in proteins, the corresponding reaction may be solely a redox process. This difference can make it difficult to obtain the appropriate E_m value in the reference system (reviewed in ref *27*).

In previous studies on the *C. beijerinckii* flavodoxin (*7*), using the HQ [for $E_{sq/hq}$ and pK_a(N5)] and OX [for E_m(FMN/$FMN^{\bullet-}$)] crystal structures, the measured $E_{sq/hq}$ and $E_{ox/sq}$ values of flavodoxins were reproduced only when the values of free FMN measured by Draper and Ingraham (*21*) were used in the reference model system. Even when other forms of crystal structures were used (e.g., $E_{sq/hq}$ calculations using structures in the OX form instead of the HQ form) along with the values measured by Anderson (*23*), the calculated values significantly differed from the measured values (*7*). To facilitate a direct comparison, we used the exact same conditions used in the previous study on the *C. beijerinckii* flavodoxin (*7*).

Influence of Atomic Charges on E_m. E_m are influenced by the protein environment, which is described by the protein dielectric volume and the charge distribution generated by the amino acids. Influence of the charges of a particular residue on E_m can be probed by setting the residue atomic charges to zero (while keeping the van der Waals volume of the corresponding atoms at the low dielectric constant of the protein and the protonation states of the other titratable residues). The influence of atomic charges is the bare effect of interactions between charges of the considered site, and the redox-active cofactor and is obtained if we calculate the E_m difference between the presence and absence of charges at the particular residue, while all other charges remain invariant.

RESULTS AND DISCUSSION

Redox Titration of $FMNH^{\bullet}/FMNH$. Using the HQ structures, we calculated the $E_{sq/hq}$ [$E_m(FMNH^{\bullet}/FMNH^-)$] value to be -444 mV for the native *D. vulgaris* flavodoxin (Figure 1), which is in excellent agreement with the values measured previously, i.e., -440 (*14*) and -443 mV (*28*) (Table 1). During the redox titration of $FMNH^{\bullet}/FMNH^-$, most titratable residues are in their standard protonation states, i.e., ionized and protonated for acidic and basic residues, respectively (Table S1 in the Supporting Information). In the present study, only Asp62, a residue in the 60s loop (Figure 2),

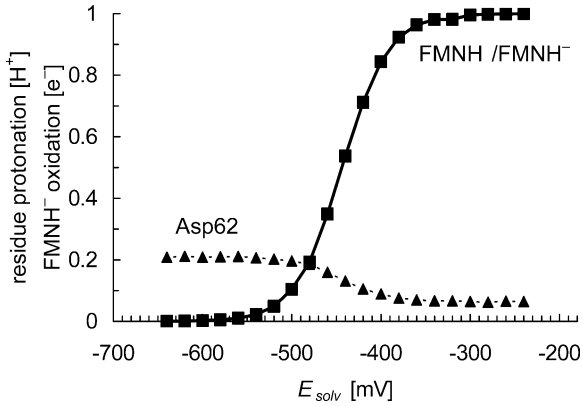

FIGURE 1: Redox titration of FMNH•/FMNH$^-$ (■) versus solvent potential (E_{solv}) and associated changes in the protonation state of Asp62 (▲) in native flavodoxin. For definitions of protonation and redox probabilities, see ref *46*.

Table 1: Influence of the Protein Environment on $E_{sq/hq}$ (Δ) of *D. vulgaris* and *C. beijerinckii* in Millivolt Units

flavodoxin	*D. vulgaris*	*C. beijerinckii*	difference[a]
$E_{sq/hq}$, experimental	−440,[b] −443[c]	−399[d]	−41, −44
$E_{sq/hq}$, calculated[e]	−444	−400	−44
$E_{sq/hq}$, uncharged protein[f]	−328	−328	0
$E_{sq/hq}$, reference[g]	−172	−172	0
Δdielectric volume[h]	−156	−156	0
Δcharge[i]	−116	−72	−44
Δbackbone	112	257	−145
(CO)	70	152	−82
(NH)	42	105	−63
Δside chain	−170	−238	68
Δphosphate	−58	−91	33

[a] $E_{sq/hq}$(*D. vulgaris*) − $E_{sq/hq}$(*C. beijerinckii*). [b] See ref *14*. [c] See ref *28*. [d] See ref *8*. [e] Values calculated in the presence of protein atomic charges. [f] Values calculated in the absence of protein atomic charges. [g] Measured values for an isolated FMN molecule in aqueous solution (*21*). [h] Contribution of protein dielectric volume to $E_{sq/hq}$: (uncharged protein) − (reference). [i] Contribution of protein atomic charges to $E_{sq/hq}$: (charged protein) − (uncharged protein).

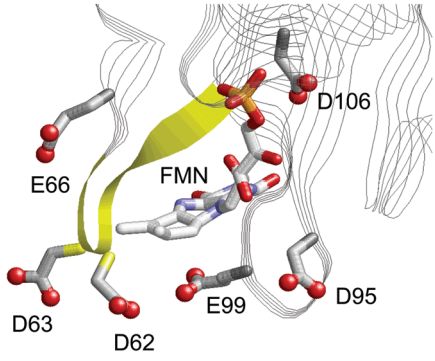

FIGURE 2: Acidic residues in the proximity of the FMN binding site. Oxygen atoms of the acidic residues are depicted as red balls. A segment of the 60s loop (residues 59–64) is depicted as a yellow ribbon, while the other part of the protein is depicted as strands.

changed its protonation state slightly in response to the changes in the redox states of FMNH•/FMNH$^-$ (Figure 1).

In the *C. beijerinckii* flavodoxin, the corresponding protonation occurs at Glu59 (protonation by ≈1 H$^+$) (*7*), which is also located in the 60s loop (Figure 3a). According to the protein sequence alignment performed with the CLUSTAL program (*29*), residues 59–64 in the *D. vulgaris* flavodoxin correspond to residues 55–60 in the *C. beijerinckii* flavodoxin (Figure 4). However, according to the geometry of the protein

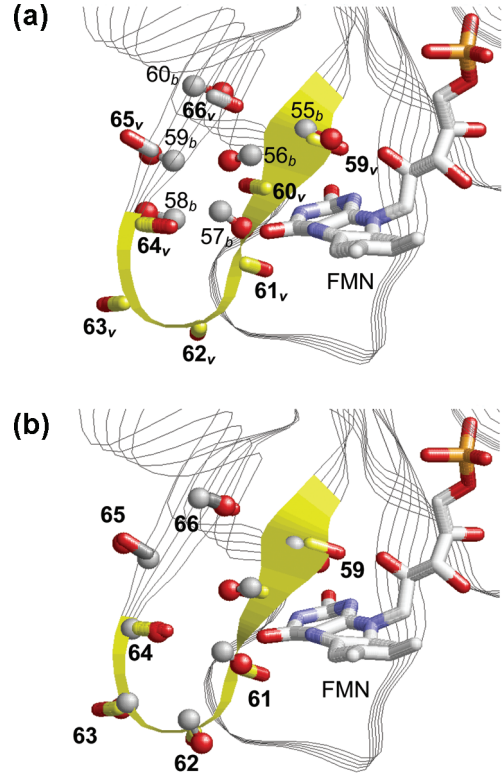

FIGURE 3: Orientation of the protein backbone carbonyl group (depicted as sticks) in a segment of the 60s loop of the native *D. vulgaris* flavodoxin (PDB code 5FX2). A comparison of the corresponding protein backbone carbonyl group (depicted as balls) of (a) the native *C. beijerinckii* flavodoxin (PDB code 5ULL) and (b) the apoflavodoxin−riboflavin complex from *D. vulgaris* (PDB code 1BU5). *v* and *b* on the labels denote the *D. vulgaris* and *C. beijerinckii* flavodoxins, respectively. The 60s loop of the native *D. vulgaris* flavodoxin is depicted as a yellow ribbon, while the other part of the protein is depicted as strands. The atomic coordinates of the two crystal structures presented were obtained by superimposing the Cα carbon atom positions with the ALIGN program (*47*). For FMN, only the molecule geometry identified in the native *D. vulgaris* flavodoxin is shown.

60's loop

D. vulgaris 51 DLVLLGCST**W** **GDDSIE**LQDD 70

C. beijerinckii 47 DILILGCSA**M** **GDEVLE**-ESE 65

FIGURE 4: Sequence alignments of the *D. vulgaris* flavodoxin with the *C. beijerinckii* flavodoxin. Residues listed in Table 4 (≈60s loop) are colored in gray.

backbone position, residues 59–61/64–66 in the *D. vulgaris* flavodoxin correspond to residues 55–57/58–60 in the *C. beijerinckii* flavodoxin and residues 62 and 63 in the *D. vulgaris* flavodoxin have no counterparts in the *C. beijerinckii* flavodoxin. Thus, Glu59 in the *C. beijerinckii* flavodoxin appears to essentially correspond to Asp62 in the *D. vulgaris* flavodoxin in terms of the protein geometry.

Mutational studies revealed that, as a result of E59Q mutation, the influence of the ionized Glu59 on $E_{sq/hq}$ is −86 mV (*30*) [−82 mV in computational studies (*7*)]. Note that protonation by ≈1 H$^+$ at Glu59 occurs when the flavin is fully reduced (*7*) and that Glu59 is ≈0.5 H$^+$ protonated (i.e., ≈50% ionized) when $E_{sq/hq}$ is measured as a midpoint potential (see Figure 3 in ref *7*). Thus, the ≈50% ionized Glu59 has an impact on $E_{sq/hq}$ (*7, 30*) in the E59Q mutant even if the fully reduced FMNH$^-$ state compensates for ≈1 H$^+$.

Table 2: Comparison between the Experimental $E_{sq/hq}$ Values of Mutant Flavodoxins and the Calculated $E_{sq/hq}$ Values of Native Flavodoxins with Protonated Acidic Residues in Millivolt Units[a]

	experimental[b]		calculated (protonation in native structure)		
	$E_{sq/hq}$	versus native[c]	$E_{sq/hq}$	versus native[c]	versus experimental[d]
native	−443	0	−444	0	−1
D62N	−426	17	−413	31	13
D63N	−431	12	−440	4	−9
E66Q	−425	18	−424	20	1
D95N	−397	46	−388	56	9
E99Q	−425	18	−434	10	−9
D106N	−429	14	−428	16	1
(sum)		(125)		(137)	
six-site mutant[e]	−350	93	−299	145	51

[a] Calculated $E_{sq/hq}$ values were obtained using the crystal structure of the native *D. vulgaris* flavodoxin (*15*) with constraints of protonation at the corresponding acidic residues. [b] Experimental values in ref *4*. [c] E_m(mutant) − E_m(native). [d] E_m(protonation in native structure) − E_m(experimental). This difference can be mainly attributed to a possible protein conformational change induced upon mutation (see the main text). [e] The multiple mutant D62N/D63N/E66Q/D95N/E99Q/D106N in ref *4*.

Table 3: Calculated $E_{sq/hq}$ Values of Native Flavodoxins with Protonated Acidic Residues and Deprotonated Basic Residues in Millivolt Units[a]

protonatation				deprotonation			
Asp	$E_{sq/hq}$	Glu	$E_{sq/hq}$	Arg	$E_{sq/hq}$	Lys	$E_{sq/hq}$
28	−443	16	−443	24	−444	3	−444
34	−444	20	−443	36	−444	87	−444
37	−442	25	−443	86	−444	111	−444
51	−444	32	−443	125	−444	113	−444
62	−413	42	−444	131	−447		
63	−440	48	−444				
69	−440	66	−424				
70	−441	79	−443				
76	−442	80	−443				
95	−388	99	−434				
106	−428	109	−435				
122	−442	110	−442				
127	−419	118	−443				
129	−438						

[a] Calculated $E_{sq/hq}$ values were obtained using the crystal structure of the native *D. vulgaris* flavodoxin (*15*) with constraints of protonation/deprotonation at the corresponding acidic residues.

On the other hand, as a result of the D62N mutation, the influence of ionized Asp62 on $E_{sq/hq}$ of the *D. vulgaris* flavodoxin is much smaller, i.e., −17 mV (*4*) (−31 mV (*4*) as a result of its protonation; Table 2). The reason for the remarkably large influence of Glu59 of the *C. beijerinckii* flavodoxin is that the carboxyl oxygen atom of Glu59 is directly involved in the hydrogen bond with the N3 nitrogen atom of FMN (O_{Glu59}−N_{FMN} distance = 3.0 Å) (*8, 31*). Thus, the influence of the D62N mutation of the *D. vulgaris* flavodoxin on $E_{sq/hq}$ is significantly small with respect to that of the E59Q mutant of the *C. beijerinckii* flavodoxin. The role of Asp62 may be more pronounced in the formation of the flavodoxin−cytochrome c_3 complex (*32*) and control of the intermolecular electron transfer rate (*33*) as suggested in former studies.

Influence of Protein Volume/Shape on $E_{sq/hq}$. The $E_{sq/hq}$ value of the *C. beijerinckii* flavodoxin [measured (*8*) and calculated (*7*) values] is ≈40 mV higher than that of the *D. vulgaris* flavodoxin. One of the remarkable findings of the present study is that the influence of uncharged protein dielectric volume (i.e., the space covered by the merged van der Waals volumes of protein atoms) on $E_{sq/hq}$ of the *D. vulgaris* flavodoxin is identical to that of the *C. beijerinckii* flavodoxin (Table 1); this fact indicates their remarkable similarity with respect to the protein volume/shape in the proximity of the FMN quinone. The calculated values of the solvent-accessible surface area (SASA) of the FMNH ring are 104 and 107 Å^2 for the *C. beijerinckii* and *D. vulgaris* flavodoxins, respectively, almost identical in the two proteins. The protein volume/shape surrounding the FMN quinone directly affects the availability of solvation (*34*) to FMN, particularly in the $FMNH^-$ state. Hence, $E_{sq/hq}$ is lower by 156 mV in the flavodoxin protein environment than in aqueous solution (Table 1) because of the absence of solvation in the $FMNH^-$ state of the protein [Note that in the present study, the protein volume is defined as the volume obtained by merging the volumes of the van der Waals spheres of all protein atoms using CHARMM (*16*) atomic radii]. Thus, it is not the protein volume/shape but the protein atomic charges that differentiate $E_{sq/hq}$ between the *D. vulgaris* and *C. beijerinckii* flavodoxins. In the subsequent discussion, we will focus on the influence of atomic charges on $E_{sq/hq}$.

Influence of Acidic Residues on $E_{sq/hq}$. The *D. vulgaris* and *C. beijerinckii* flavodoxins possess more acidic residues (30 and 28) than basic residues (11 and 12, respectively). Ludwig et al. (*35*) proposed that negatively charged acidic residues are more important than the phosphate group in determining the $E_{sq/hq}$ value. In agreement with their proposal, in the *D. vulgaris* and *C. beijerinckii* flavodoxins, the influence of side chains on $E_{sq/hq}$ ($E_{sq/hq}$ downshift of ≈170–240 mV), presumably because of acidic residues, is considerably larger than that of the phosphate group ($E_{sq/hq}$ downshift of ≈60–90 mV) (Table 1).

In studies on the *D. vulgaris* flavodoxin (*4*), mutations of acidic residues (Asp and Glu located within 13 Å of FMN) to uncharged residues (i.e., Asn and Gln, respectively) resulted in an upshift in the $E_{sq/hq}$ value (Table 2). In the present study, the influence of protonation of these acidic residues on $E_{sq/hq}$ was investigated using the crystal structure of the native *D. vulgaris* flavodoxin. Using the geometry of the native crystal structure, we could focus only on the actual influence of the ionized acidic groups on $E_{sq/hq}$ in the native flavodoxin, while excluding the influence of the structural changes induced by mutations.

The calculated shift in the $E_{sq/hq}$ value because of the protonation of each single acidic residue is very close to the measured shift in $E_{sq/hq}$ upon a single mutation (*4*) (Table 2). In the present calculation, Asp95 had the largest impact on the $E_{sq/hq}$ value (56 mV, Table 2) among the six acidic residues investigated [Asp62, Asp63, Glu66, Asp95, Glu99, and Asp106 (Figure 2)]; this is in good agreement with the $E_{sq/hq}$ shift (46 mV, Table 2) experimentally measured in mutational studies (*4*). Except the six acidic residues, protonation of Asp127 is notable, yielding the shift of 25 mV in $E_{sq/hq}$ (Table 3).

Zhou and Swenson (*4*) generated a mutant flavodoxin in which the six acidic residues were mutated to uncharged residues simultaneously (six-site mutant). The measured $E_{sq/hq}$ value of the six-site mutant is −350 mV (*4*). On the other hand, the corresponding $E_{sq/hq}$ value of the six-site protonated native protein is −299 mV (Table 2). The remaining

Table 4: Influence of the Protein Backbone of the 60s Loop on $E_{sq/hq}$ of *D. vulgaris* and *C. beijerinckii* in Millivolt Units

D. vulgaris							*C. beijerinckii*			
	native			riboflavin complex				native		
residue[a]	CO	NH	total	CO	NH	total	residue[a]	CO	NH	total
59	−21	12	−9	−46	11	−35	55	−20	6	−14
60	−1	−11	−12	3	−10	−7	56	6	−10	−4
61	−52	−28	−80	−21	−20	−41	57	−30	−24	−54
62	−1	−10	−11	0	−6	−6				
63	5	−5	0	0	−2	−2				
64	−10	−1	−11	−9	−2	−11	58	25	−7	18
65	14	0	14	14	3	17	59	22	36	58
66	−20	6	−14	−17	3	−14	60	−17	3	−14
total	−86	−37	−123	−76	−23	−99		−14	4	−10

[a] According to the protein sequence alignment performed with the CLUSTAL program (*29*), residues 59–64 in the *D. vulgaris* flavodoxin correspond to residues 55–60 in the *C. beijerinckii* flavodoxin. However, according to the geometry of the protein backbone position, residues 59–61/64–66 in the *D. vulgaris* flavodoxin correspond to residues 55–57/58–60 in the *C. beijerinckii* flavodoxin, and residues 62 and 63 in the *D. vulgaris* flavodoxin have no counterparts in the *C. beijerinckii* flavodoxin.

discrepancy of ≈50 mV in the $E_{sq/hq}$ upshift between the two flavodoxins (i.e., the six-site mutant and six-site protonated flavodoxins) is most likely due to discrepancies in protein structures of the six-site protonated native protein (i.e., model structure) and the actual six-site mutant. This type of conformational change has a tendency to compensate for induced dramatic changes in the protein net charge (see refs *18–20 and 36*). This type of conformational change will be much smaller in the case of a single mutation because the change in the protein charge is more moderate. Hence, an unusually large increase of +6 net charge upon the six-site mutation appears to induce a large protein conformational change (and a possible change in the protonation pattern of surrounding residues), compensating for the influence of simultaneous elimination of the −6 charge.

We also investigated influences of deprotonation of the basic residues by deprotonating only the focusing residues. Because most of the basic residues are away from the flavin binding site (Figure S1 in the Supporting Information), influences of deprotonation of basic residues on $E_{sq/hq}$ were considerably small with respect to those of the protonation of acidic residues (Table 3). In addition, deprotonation of the basic residues often induces new protonation patterns of the titratable residues in the protein. For instance, Arg125 and Asp106 are located in the proximity of the flavin binding site. When we deprotonated Arg125, we observed that Asp106 became protonated by ≈0.5 H^+. Note that we constrained the protonation state of the only focusing residue, while the protonation states of other residues are fully equilibrated.

Compensation of the Influence of the Anionic Group on $E_{sq/hq}$ by the Protein Backbone. The $E_{sq/hq}$ value of the *D. vulgaris* flavodoxin [−440 mV (*14*) and −443 mV (*28*)] is ≈40 mV lower than that of the *C. beijerinckii* flavodoxin [−399 mV (*8*)]. In contrast, the $E_{sq/hq}$ downshift because of the protein side chains and the FMN 5′-phosphate group in the *D. vulgaris* flavodoxin is ≈100 mV smaller than that in the *C. beijerinckii* flavodoxin (Table 1) [Note that protein side chain refers to uncharged, acidic, and basic groups. However, in the downshift in $E_{sq/hq}$ because of the protein side chains (Table 1), the influence of acidic residues on $E_{sq/hq}$ appears to be predominant. Therefore, in the following text, we refer to "protein side chain" influence as "acidic group" influence]. Hence, protein side chains (i.e., acidic residues) and the phosphate group are not directly responsible for the lower $E_{sq/hq}$ value of the *D. vulgaris* flavodoxin as compared to the *C. beijerinckii* flavodoxin.

This issue can be addressed by a dramatic difference in the influence of the protein backbone charge on $E_{sq/hq}$ between the two flavodoxins (Table 1). In the *C. beijerinckii* flavodoxin, the acidic groups cause a downshift of 329 mV in $E_{sq/hq}$; this is compensated to a great extent by the upshift of 257 mV in $E_{sq/hq}$ exerted by the protein backbone (*7*). In contrast, the upshift in $E_{sq/hq}$ exerted by the protein backbone of the *D. vulgaris* flavodoxin is only 112 mV, which is 145 mV smaller than the corresponding upshift in the *C. beijerinckii* flavodoxin (Table 1). Thus, the protein backbone is clearly linked to the difference in $E_{sq/hq}$ values between the *D. vulgaris* and *C. beijerinckii* flavodoxins.

Protein Backbone Influence and Riboflavin Binding. Riboflavin, which lacks the 5′-phosphate group of FMN quinone, can bind with the *D. vulgaris* apoflavin protein, but it fails to bind with the *C. beijerinckii* apoflavin protein (*12, 37*). Interestingly, circular dichroism spectroscopic studies indicated that the apoflavodoxin that binds riboflavin (e.g., the *D. vulgaris* apoflavin) has a more apolar protein environment around the FMN binding site as compared to that in the apoflavodoxin that fails to bind riboflavin (e.g., the *C. beijerinckii* apoflavin) (*37*). In the present study, the protein backbone influence on $E_{sq/hq}$ in the *D. vulgaris* flavodoxin (112 mV) is considerably smaller than that in the *C. beijerinckii* flavodoxin (257 mV) (Table 1). In general, the protein backbone dipole is one of the key factors that determine the polarities of the protein environment (e.g., see refs *38–42*). Hence, the protein backbone influence may be a factor that determines the polarity of the FMN binding sites of the two flavodoxins observed in circular dichroism spectroscopic studies (*37*) and the ability of binding riboflavin.

Protein Backbone Conformation of the 60s Loop. Both the *D. vulgaris* and *C. beijerinckii* flavodoxins possess the 60s loop in the proximity of the FMN quinone (Figure 3a). The influence of the protein backbone of a segment in the 60s loop (59–66 in the *D. vulgaris* flavodoxin and 55–60 in the *C. beijerinckii* flavodoxin) on $E_{sq/hq}$ differs (−123 and −10 mV, respectively, Table 4) by more than 100 mV between the two flavodoxins. Indeed, this difference of 5005 mV (=|−123 − (−10)|, Table 4) in $E_{sq/hq}$ attributed to the 60s loop forms a major part of the net difference in the protein backbone influence on $E_{sq/hq}$ (257 – 112 = 145 mV, Table 1) between the two flavodoxins. Although the actual

influence of the 60s loop on $E_{sq/hq}$ has never been measured directly, there are experimental evidence that the protein conformation of the 60s loop is related to the redox state of the FMN quinone (*5, 8, 9*) or riboflavin affinity to the apoflavodoxin (*12, 43, 44*) (however, for ref *12*, see the subsequent discussion).

Hence, the difference in the protein backbone conformation of the 60s loop is a key factor with respect to the difference in the net protein backbone influence on $E_{sq/hq}$ and, therefore, the $E_{sq/hq}$ difference between *D. vulgaris* and *C. beijerinckii* flavodoxins. Note that a large influence of the protein backbone of the loop region near the redox-active group in proteins has also been reported in heme proteins (*41*).

Understanding the Upshift of 180 mV in $E_{sq/hq}$ upon Apoflavodoxin−Riboflavin Complex Formation. The measured $E_{sq/hq}$ value of the apoflavodoxin−-riboflavin complex from *D. vulgaris* (that lacks the negatively charged 5′-phosphate group) was 180 mV greater than that of the native flavodoxin (*14*). The reasons for the 180 mV upshift in $E_{sq/hq}$ have been discussed as follows:

(a) Negatively Charged 5′-Phosphate Group. On the basis of theoretical studies, Moonen et al. (*10*) concluded that the negatively charged phosphate group was responsible for the 180 mV downshift in $E_{sq/hq}$ of the native flavodoxin. Thus, the negatively charged 5′-phosphate group was often speculated to be a major factor that significantly affected the $E_{sq/hq}$ values of flavodoxins (*11*). However, in the present study, the calculated downshift of ≈60 mV in $E_{sq/hq}$ of the *D. vulgaris* flavodoxin (Table 1) is considerably lower than 180 mV. This also holds true for the *C. beijerinckii* flavodoxin, where the corresponding downshift in $E_{sq/hq}$ is calculated to be ≈90 mV (*7*).

The difference of 33 mV in influence of the phosphate group on $E_{sq/hq}$ (Table 1) is due to their different protonation states: the phosphate groups were almost mono- and dianionic in the *D. vulgaris* and *C. beijerinckii* flavodoxins, respectively. The different charge states are due to the different hydrogen-bonding pattern for the phosphate group. There are four conserved Ser and Thr residues that are at an hydrogen-bonding distance from the oxygen atoms of the phosphate group, namely, Ser10, Thr12, Thr15, and Ser58 in the *D. vulgaris* flavodoxin (Ser7, Thr9, Thr12, and Ser54 in the *C. beijerinckii* flavodoxin). The hydroxyl groups of Ser7 and the backbone amide group of Thr12 form hydrogen bonds with the phosphate oxygen atom (O3P) in the *C. beijerinckii* flavodoxin (PDB code 5ULL). The corresponding hydrogen bonds (from the Ser10 side chain and the Thr12 backbone) is also observed in the *D. vulgaris* flavodoxin (PDB code 5FX2, where the corresponding phosphate oxygen atom is O1P).

In the *D. vulgaris* flavodoxin, the hydroxyl group of Thr15 is at a hydrogen-bonding distance with the phosphate O1P atom (O−O distance of 2.9 Å). However, this group does not form a hydrogen bond with the O1P atom probably because the O1P atom has already possessed two hydrogen bonds (Figure 5a). In particular, the hydrogen-bond distance between the hydroxyl oxygen atom of Ser10 and O1P is 2.1 Å, stabilizing the ionized state of the phosphate significantly. Thus, only the second hydrogen bond from the amide group of Thr15 (N−O distance of 2.7 Å) can probably be added energetically to the O1P atom in the *D. vulgaris* flavodoxin.

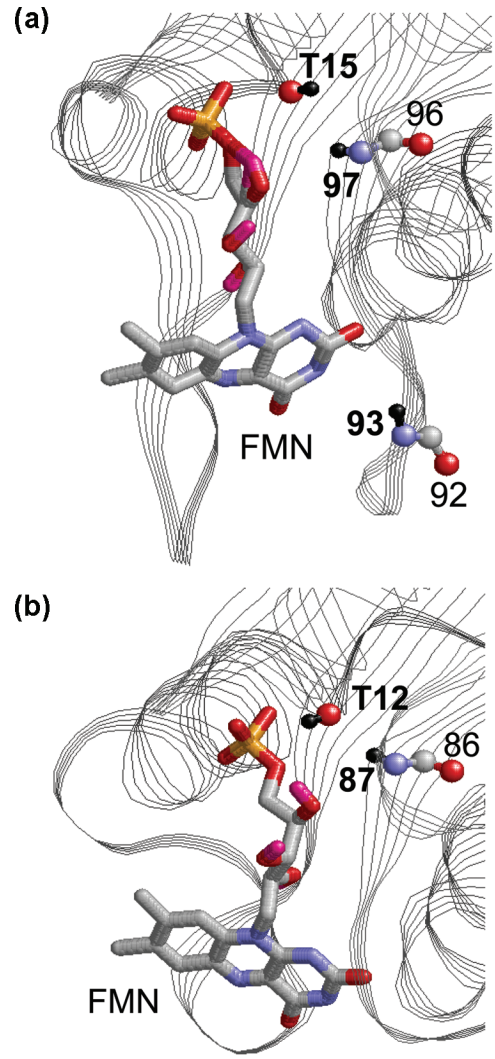

FIGURE 5: (a) Orientation of the hydroxyl group of Thr15, the backbone carbonyl groups of Gly92 and Ser96, and the backbone amide groups of Cys93 and Ser97 (depicted as balls) in the native *D. vulgaris* flavodoxin (PDB code 5FX2). (b) Orientation of the hydroxyl group of Thr12, the backbone carbonyl group of Gly86, and the backbone amide group of Ser87 in the native *C. beijerinckii* flavodoxin (PDB code 5ULL). Polar hydrogen atoms of the Thr side chains and the protein backbone amide groups are depicted as black balls.

On the other hand, the corresponding hydroxyl group of Thr12 forms a hydrogen bond with the O3P atom in the *C. beijerinckii* flavodoxin (Figure 5b). It appears that Thr12 is forced to form a hydrogen bond with the O3P atom because of the presence of the backbone amide group of Ser87 that donates a hydrogen bond with Thr12 (N−O distance of 3.3 Å). Ser87 in the *C. beijerinckii* flavodoxin is also conserved in the *D. vulgaris* flavodoxin as Ser97. However, Ser97 in the *D. vulgaris* flavodoxin is considerably away from the O1P atom (≈15 Å). Indeed, Ser87 in the *C. beijerinckii* flavodoxin belongs to a β-sheet segment (i.e., residues 81–88), while Ser97 in the *D. vulgaris* flavodoxin does not belong to the corresponding β sheet (i.e., residues 87–94). In the *D. vulgaris* flavodoxin, the backbone amide group of Cys93 is the closest to the hydroxyl group of Thr15, but this amide group cannot form a hydrogen bond with Thr15 because of its inappropriate orientation (Figure 5b). In summary, Thr15 does not form a hydrogen bond with the phosphate O1P atom in the *D. vulgaris* flavodoxin, while

Table 5: Calculated $E_{sq/hq}$ Values for the Apoflavodoxin−Riboflavin Complex in Millivolt Units

flavodoxin	FMN	riboflavin	crystal structure	PDB code
$E_{sq/hq}$, experimental	−440[a], −443[b]	−262[a]		
$E_{sq/hq}$, calculated	−444	−400[c]	HQ[d]	5FX2[d]
	−407	−357[c]	OX[d]	3FX2[d]
	nd	−468	riboflavin complex (OX)[e]	1BU5[e]

[a] See ref *14*. $E_{sq/hq}$ of the apoflavodoxin−riboflavin complex was measured at pH 6.5. [b] See ref *28*. [c] To calculate the $E_{sq/hq}$ value of the apoflavodoxin−riboflavin complex, the atomic coordinates of the 5′-phosphate group were deleted from those of the original crystal structure (i.e., the model structure obtained from the atomic coordinates of native flavodoxin). [d] See ref *15*. [e] See ref *12*. Note that the HQ form is not yet available.

Thr12 forms a hydrogen bond with the phosphate O3P atom in the *C. beijerinckii* flavodoxin because of the presence of the backbone amide group of Ser87. This difference is responsible for the difference of 33 mV in influence of the phosphate group on $E_{sq/hq}$ by altering the charge states of the phosphate group in the two proteins.

(b) Deletion of the Phosphate Group. We also calculated the $E_{sq/hq}$ value using the native flavodoxin crystal structure (*15*) and deleting the 5′-phosphate group from the atomic coordinates (i.e., phosphate-deleted flavodoxin). Upon deletion of the 5′-phosphate group, we observed an upshift of ≈50 mV in $E_{sq/hq}$ in the *D. vulgaris* flavodoxin (Table 5), which is essentially at the same level as the "Δphosphate" value in Table 1 [see the Supporting Information for a discussion of the difference from the corresponding value (58 mV) in Table 1].

Interestingly, in studies on the *D. vulgaris* mutants T12H and N14H, the $E_{sq/hq}$ values were increased by 28 and 15 mV relative to that of the native flavodoxin (*13*). In these mutants, the charge of the 5′-phosphate group was probably compensated for by the introduction of His residues because they are likely to be doubly protonated (i.e., positively charged) because of the negative charge of the 5′-phosphate group. Although the observed $E_{sq/hq}$ shifts (*13*) were somewhat less pronounced than that calculated in this study because of the different systems and approaches, both results suggest that the 5′-phosphate group is not a major factor in determining the $E_{sq/hq}$ value. Hence, the absence of the 5′-phosphate group in the apoflavodoxin−riboflavin complex appears to be responsible for the upshift of ≈50 mV in $E_{sq/hq}$, but it is very small to account for the entire upshift of 180 mV (*14*) in $E_{sq/hq}$.

(c) 60s Loop Movement. In the crystal structure of the apoflavodoxin−riboflavin complex from *D. vulgaris* (*12*), the 60s loop moved away from FMN with respect to the native flavodoxin structure (Figure 3b). Therefore, Walsh et al. (*12*) speculated that the 60s loop movement was responsible for the upshift of 180 mV in $E_{sq/hq}$ upon apoflavodoxin−riboflavin complex formation. To test this hypothesis, we calculated the $E_{sq/hq}$ value using the crystal structure of the apoflavin−riboflavin complex from *D. vulgaris* reported by Walsh et al. (*12*). However, the calculated $E_{sq/hq}$ value is −468 mV, which is, in turn, a downshift from the $E_{sq/hq}$ value of the native flavodoxin (Table 5).

To investigate further details, we also compared the influence of the protein backbone of the 60s loop on $E_{sq/hq}$ between the native (*15*) flavodoxin and the apoflavodoxin−riboflavin complex (*12*). We observed a notable difference in the influence of the Gly61 protein backbone on $E_{sq/hq}$ between the two protein forms (Table 4). The position of the protein backbone carbonyl group at Gly61 with respect to the FMN ring is indeed different between the two crystal structures (Figure 3b). However, this difference appears to be partially compensated by the influences of the other protein backbones (e.g., Thr59 in Table 4). Consequently, the net influence of the 60s loop on $E_{sq/hq}$ is essentially at the same level in both the native flavodoxin and the apoflavodoxin−riboflavin complex (−123 and −99 mV, respectively, Table 4).

Hence, the present result demonstrates that the 60s loop movement identified in the apoflavodoxin−riboflavin complex (*12*) has little relation with the observed upshift of 180 mV in $E_{sq/hq}$ (*14*). Nevertheless, it should also be noted that the currently available crystal structure of the apoflavodoxin−riboflavin complex is its OX form (that does not contain $FMNH^{\bullet}/FMNH^{-}$) because of the difficulty in obtaining the HQ form (*12*). Therefore, a possible role of the 60s loop movement in contributing to the $E_{sq/hq}$ shift may not be completely excluded until the relevant crystal structure in the HQ form is investigated. It appears that at least in the currently available crystal structure (*12*), the protein geometry has little relation with the experimentally determined $E_{sq/hq}$ value (*14*).

As discussed above, the 5′-phosphate group is responsible for the upshift of only ≈50 mV in $E_{sq/hq}$ in calculations using the geometry of the native flavodoxin crystal structure (Table 5). The 60s loop movement observed in the currently available crystal structure of the apoflavodoxin−riboflavin complex (*12*) has little relation with the upshift in $E_{sq/hq}$.

CONCLUSION

Using the crystal structure in the HQ form, the $E_{sq/hq}$ value for the *D. vulgaris* flavodoxin was calculated to be −444 mV, which is in good agreement with the experimental values (*14, 28*). The calculated influence of acidic residues on $E_{sq/hq}$ matches the experimentally measured $E_{sq/hq}$ values of each corresponding mutant flavodoxin (*4*). Influences of deprotonation of basic residues on $E_{sq/hq}$ were considerably small with respect to those of protonation of acidic residues. Influences of the protein backbone conformation of the 60s loop on the redox potentials have been experimentally suggested for the *D. vulgaris* (*15*) and *C. beijerinckii* (*8, 9, 30, 45*) flavodoxins. The present computational study confirms these experimental results and suggests that the $E_{sq/hq}$ difference between the *D. vulgaris* and *C. beijerinckii* flavodoxins can be best explained by the lower compensation of the side-chain influence by the backbone influence in the *D. vulgaris* flavodoxin than in the *C. beijerinckii* flavodoxin. In particular, the influence of the protein backbone of a segment in the 60s loop (59–66 in the *D. vulgaris* flavodoxin and 55–60 in the *C. beijerinckii* flavodoxin) on $E_{sq/hq}$ differs by more than 100 mV. Hence, the protein backbone conformation of the 60s loop is a key factor in determining the difference in $E_{sq/hq}$ between *D. vulgaris* and *C. beijerinckii* flavodoxins. In the native flavodoxin, the 5′-phosphate group is responsible for a downshift of only ≈50 mV in $E_{sq/hq}$. The 60s loop movement identified in the apoflavodoxin−

riboflavin complex (*12*) does not cause an upshift in $E_{sq/hq}$. Currently, the lowered flavin cofactor binding in the apoflavodoxin−riboflavin complex (*13*) is most likely the major factor for the experimentally observed upshift of 180 mV (*14*) in $E_{sq/hq}$.

ACKNOWLEDGMENT

I thank Dr. Arieh Warshel and Dr. Ernst-Walter Knapp for useful discussions.

SUPPORTING INFORMATION AVAILABLE

Further analysis of the influence of the 5′-phosphate group and protonation states of titratable sites in flavodoxins (Table S1). This material is available free of charge via the Internet at http://pubs.acs.org.

REFERENCES

1. Niemz, A., and Rotello, V. M. (1999) From enzyme to molecular device. Exploring the interdependence of redox and molecular recognition. *Acc. Chem. Res. 32*, 44–52.
2. Bhattacharyya, S., Stankovich, M. T., Truhlar, D. G., and Gao, J. (2007) Combined quantum mechanical and molecular mechanical simulations of one- and two-electron reduction potentials of flavin cofactor in water, medium-chain acyl-CoA dehydrogenase, and cholesterol oxidase. *J. Phys. Chem. A 111*, 5729–5742.
3. Yalloway, G. N., Mayhew, S. G., Malthouse, J. P. G., Gallagher, M. E., and Curley, G. P. (1999) pH-dependent spectroscopic changes associated with the hydroquinone of FMN in flavodoxins. *Biochemistry 38*, 3753–3762.
4. Zhou, Z., and Swenson, R. P. (1995) Electrostatic effects of surface acidic amino acid residues on the oxidation-reduction potentials of the flavodoxin from *Desulfovibrio vulgaris* (Hildenborough). *Biochemistry 34*, 3183–3192.
5. McCarthy, A. A., Walsh, M. A., Verma, C. S., O'Connell, D. P., Reinhold, M., Yalloway, G. N., d'Arcy, D., Higgins, T. M., Voordouw, G., and Mayhew, S. G. (2002) Crystallographic investigation of the role of aspartate 95 in the modulation of the redox potentials of *Desulfovibrio vulgaris* flavodoxin. *Biochemistry 41*, 10950–10962.
6. Popovic, D. M., Zmiric, A., Zaric, S. D., and Knapp, E.-W. (2002) Energetics of radical transfer in DNA photolyase. *J. Am. Chem. Soc. 124*, 3775–3782.
7. Ishikita, H. (2007) Contributions of protein environment to redox potentials of quinones in flavodoxins from *Clostridium beijerinckii*. *J. Biol. Chem. 282*, 25240–25246.
8. Ludwig, M. L., Pattridge, K. A., Metzger, A. L., Dixon, M. M., Eren, M., Feng, Y., and Swenson, R. P. (1997) Control of oxidation−reduction potentials in flavodoxin from *Clostridium beijerinckii*: The role of conformation changes. *Biochemistry 36*, 1259–1280.
9. Kasim, M., and Swenson, R. P. (2000) Conformational energetics of a reverse turn in the *Clostridium beijerinckii* flavodoxin is directly coupled to the modulation of its oxidation−reduction potentials. *Biochemistry 39*, 15322–15332.
10. Moonen, C. T. W., Vervoort, J., and Müller, F. (1984) In *Flavins and Flavoproteins* (Bray, R. C., Engel, P. C., and Mayhew, S. G., Eds.) pp 493–496, Walter de Gruyter and Co., Berlin, Germany.
11. Pueyo, J. J., Curley, G. P., and Mayhew, S. G. (1996) Kinetics and thermodynamics of the binding of riboflavin, riboflavin 5′-phosphate and riboflavin 3′,5′-bisphosphate by apoflavodoxins. *Biochem. J. 313*, 855–861.
12. Walsh, M. A., McCarthy, A., O'Farrell, P. A., McArdle, P., Cunningham, P. D., Mayhew, S. G., and Higgins, T. M. (1998) X-ray crystal structure of the *Desulfovibrio vulgaris* (Hildenborough) apoflavodoxin−riboflavin complex. *Eur. J. Biochem. 258*, 362–371.
13. Zhou, Z., and Swenson, R. P. (1996) Evaluation of the electrostatic effect of the 5′-phosphate of the flavin mononucleotide cofactor on the oxidation−reduction potentials of the flavodoxin from *Desulfovibrio vulgaris* (Hildenborough). *Biochemistry 35*, 12443–12454.
14. Curley, G. P., Carr, M. C., Mayhew, S. G., and Voordouw, G. (1991) Redox and flavin-binding properties of recombinant flavodoxin from *Desulfovibrio vulgaris* (Hildenborough). *Eur. J. Biochem. 202*, 1091–1100.
15. Watt, W., Tulinsky, A., Swenson, R. P., and Watenpaugh, K. D. (1991) Comparison of the crystal structures of a flavodoxin in its three oxidation states at cryogenic temperatures. *J. Mol. Biol. 218*, 195–208.
16. Brooks, B. R., Bruccoleri, R. E., Olafson, B. D., States, D. J., Swaminathan, S., and Karplus, M. (1983) CHARMM: A program for macromolecular energy minimization and dynamics calculations. *J. Comput. Chem. 4*, 187–217.
17. Bashford, D., and Karplus, M. (1990) pK_a's of ionizable groups in proteins: Atomic detail from a continuum electrostatic model. *Biochemistry 29*, 10219–10225.
18. Ishikita, H., and Knapp, E.-W. (2005) Induced conformational change upon Cd^{2+} binding at photosynthetic reaction centers. *Proc. Natl. Acad. Sci. U.S.A. 102*, 16215–16220.
19. Ishikita, H., and Knapp, E.-W. (2005) Energetics of proton transfer pathways in reaction centers from *Rhodobacter sphaeroides*: The Glu-H173 activated mutants. *J. Biol. Chem. 280*, 12446–12450.
20. Ishikita, H. (2007) Modulation of the protein environment in the hydrophilic pore of the ammonia transporter protein AmtB upon the GlnK protein binding. *FEBS Lett. 581*, 4293–4297.
21. Draper, R. D., and Ingraham, L. L. (1968) A potentiometric study of the flavin semiquinone equilibrium. *Arch. Biochem. Biophys. 125*, 802–808.
22. Kumler, W. D., and Eiler, J. J. (1943) The acid strength of mono- and diesters of phosphoric acid. The *n*-alkyl esters from methyl to butyl, the esters of biological importance, and the natural guanidine phosphoric acids. *J. Am. Chem. Soc. 65*, 2355–2361.
23. Anderson, R. F. (1983) Energetics of the one-electron reduction steps of riboflavin, FMN and FAD to their fully reduced forms. *Biochim. Biophys. Acta 722*, 158–162.
24. Mayhew, S. G. (1999) The effects of pH and semiquinone formation on the oxidation−reduction potentials of flavin mononucleotide. *Eur. J. Biochem. 265*, 698–702.
25. Michaelis, L. (1935) Semiquinones, the intermediate steps of reversible organic oxidation−reduction. *Chem. Rev. 16*, 243–286.
26. Williamson, G., and Edmondson, D. E. (1985) Effect of pH on oxidation−reduction potentials of 8α-*N*-imidazole-substituted flavins. *Biochemistry 24*, 7790–7797.
27. Gunner, M. R., Mao, J.-J., Song, Y.-F., and Kim, J. (2006) Factors influencing the energetics of electron and proton transfers in proteins. What can be learned from calculations? *Biochim. Biophys. Acta 1757*, 942–968.
28. Swenson, R. P., and Krey, G. D. (1994) Site-directed mutagenesis of tyrosine-98 in the flavodoxin from *Desulfovibrio vulgaris* (Hildenborough): Regulation of oxidation−reduction properties of the bound FMN cofactor by aromatic, solvent, and electrostatic interactions. *Biochemistry 33*, 8505–8514.
29. Higgins, D. G., Thompson, J. D., and Gibson, T. J. (1996) Using CLUSTAL for multiple sequence alignments. *Methods Enzymol. 266*, 383–402.
30. Bradley, L. H., and Swenson, R. P. (1999) Role of glutamate-59 hydrogen bonded to N(3)H of the flavin mononucleotide cofactor in the modulation of the redox potentials of the *Clostridium beijerinckii* flavodoxin. Glutamate-59 is not responsible for the pH dependency but contributes to the stabilization of the flavin semiquinone. *Biochemistry 38*, 12377–12386.
31. Bradley, L. H., and Swenson, R. P. (2001) Role of hydrogen bonding interactions to N(3)H of the flavin mononucleotide cofactor in the modulation of the redox potentials of the *Clostridium beijerinckii* flavodoxin. *Biochemistry 40*, 8686–8695.
32. Stewart, D. E., LeGall, J., Moura, I., Moura, J. J. G., Peck, H. D., Xavier, A. V. J., Weiner, P. K., and Wampler, J. E. (1988) A hypothetical model of the flavodoxin−tetraheme cytochrome c_3 complex of sulfate-reducing bacteria. *Biochemistry 27*, 2444–2450.
33. Feng, Y., and Swenson, R. P. (1997) Evaluation of the role of specific acidic amino acid residues in electron transfer between the flavodoxin and cytochrome c_3 from *Desulfovibrio vulgaris* [Hildenborough]. *Biochemistry 36*, 13617–13628.
34. Kato, M., Pisliakov, A. V., and Warshel, A. (2006) Barrier for proton transport in aquaporins as a challenge for electrostaatic models: The role of protein relaxation in mutational calculations. *Proteins 64*, 829–844.
35. Ludwig, M. L., Schopfer, L. M., Metzger, A. L., Pattridge, K. A., and Massey, V. (1990) Structure and oxidation−reduction behavior of 1-deaza-FMN flavodoxins: Modulation of redox potentials in flavodoxins. *Biochemistry 29*, 10364–10375.

36. Sebban, P., Maróti, P., Schiffer, M., and Hanson, D. K. (1995) Electrostatic dominoes: Long distance propagation of mutational effects in photosynthetic reaction centers of *Rhodobacter capsulatus*. *Biochemistry 34*, 8390–8397.
37. D'Anna, J. A. J., and Tollin, G. (1972) Studies of flavin−protein interaction in flavoproteins using protein fluorescence and circular dichroism. *Biochemistry 11*, 1073–1080.
38. Muegge, I., Schweins, T., Langen, R., and Warshel, A. (1996) Electrostatic control of GTP and GDP binding in the oncoprotein p21ras. *Structure 4*, 475–489.
39. Vagedes, P., Rabenstein, B., Aqvist, J., Marelius, J., and Knapp, E.-W. (2000) The deacylation step of acetylcholinesterase: Computer simulation studies. *J. Am. Chem. Soc. 122*, 12254–12262.
40. Kim, J., Mao, J., and Gunner, M. R. (2005) Are acidic and basic groups in buried proteins predicted to be ionized? *J. Mol. Biol. 348*, 1283–1298.
41. Ishikita, H., and Knapp, E.-W. (2005) Redox potential of cytochrome c550 in the cyanobacterium *Thermosynechococcus elongatus*. *FEBS Lett. 579*, 3190–3194.
42. Spassov, V. Z., Yan, L., and Flook, P. K. (2007) The dominant role of side-chain backbone interactions in structural realization of amino acid code. ChiRotor: A side-chain prediction algorithm based on side-chain backbone interactions. *Protein Sci. 16*, 494–506.
43. Murray, T. A., Foster, M. P., and Swenson, R. P. (2003) Mechanism of flavin mononucleotide cofactor binding to the *Desulfovibrio vulgaris* flavodoxin. 2. Evidence for cooperative conformational changes involving tryptophan 60 in the interaction between the phosphate- and ring-binding subsites. *Biochemistry 42*, 2317–2327.
44. Muralidhara, B. K., Chen, M., Ma, J., and Wittung-Stafshede, P. (2005) Effect of inorganic phosphate on FMN binding and loop flexibility in *Desulfovibrio desulfuricans* apo-flavodoxin. *J. Mol. Biol. 349*, 87–97.
45. Kasim, M., and Swenson, R. P. (2001) Alanine-scanning of the 50's loop in the *Clostridium beijerinckii* flavodoxin: Evaluation of additivity and the importance of interactions provided by the main chain in the modulation of the oxidation−reduction potentials. *Biochemistry 40*, 13548–13555.
46. Ullmann, G. M., and Knapp, E.-W. (1999) Electrostatic models for computing protonation and redox equilibria in proteins. *Eur. Bophys. J. 28*, 533–551.
47. Cohen, G. E. (1997) ALIGN: A program to superimpose protein coordinates, accounting for insertions and deletions. *J. Appl. Crystallogr. 30*, 1160–1161.

BI702151K